



Unraveling the flexural behavior of concrete and compare with innovative fea investigations

Naveen Arasu Anbarasu¹, Lakshmi Keshav², Kalyana Chakravarthy Polichetty Raja³,
Vivek Sivakumar⁴

¹CMS College of Engineering and Technology, Department of Civil Engineering. Coimbatore, Tamilnadu, India.

²Velagapudi Ramakrishna Siddhartha Engineering College, Department of Civil Engineering. Vijayawada, Andhra Pradesh, India.

³Vels Institute of Science, Technology & Advanced Studies, School of Engineering, Department of Civil Engineering. Chennai, Tamilnadu, India.

⁴GMR Institute of Technology, Department of Civil Engineering. Rajam, Andhra Pradesh, India.

e-mail: naveenanbu07@gmail.com, lakshmikeshav@ursiddhartha.ac.in, kalyanstructure12@gmail.com, 1717vivek@gmail.com

ABSTRACT

Modern structural issues require multi-functional concrete, and demand for it is enriched. The advancement of nano engineering technology plays a major role in the cementitious materials namely flyash, silica fume and graphene oxide. In this research varying percentages from 0 to an increment of 0.01% upto 0.05% of graphene oxide and 20% of flyash and silica fume together is used by weight of ordinary Portland cement to obtain high strength. To unravel the complex flexural behavior of concrete structures by integrating static load tests and the best mix is compared with advanced Finite Element Analysis (FEA) techniques, specifically utilizing ANSYS. The study investigates the structural response under static loading, focusing on vital parameters such as load deflection, ductility factor, stiffness factor, energy absorption capacity, and energy index. The examination of these factors provides comprehensive insights into the material's deformation characteristics and resilience in flexural conditions. The incorporation of innovative materials fly ash, silica fume, and graphene oxide into the concrete matrix are potential to enhance concrete properties, and their impact on flexural behavior. The 0.04% of graphene oxide is superior in all aspects flexural behavior and it is compared with FEA model (ANSYS).

Keywords: Graphene oxide; silica fume; flyash; strength; flexural behavior and finite element analysis.

1. INTRODUCTION

The primary characteristics of this method are increased strength, high early compressive strength, high flexural strength, and high elastic modulus. The qualities of concrete, environmental output, and energy conservation are all improved at the nanoscale level. As a result, nanotechnology contributes to increased concrete strength, decreased overall porosity, and accelerated C-S-H gel formation [1]. The incorporation of fly ash, SF, and graphene oxide into concrete, recognized as pozzolanic admixtures, delivers a substantial enrichment in the physical properties of the material. When combined with superplasticizers, these additives result in a significant boost in flexural strength, imparting greater robustness and durability to the concrete structures [2]. The introduction of graphene oxide into the concrete mixture contributes to an enhanced level of durability by effectively reducing permeability. This reduction in permeability is attributed to the heightened pozzolanic activity within the concrete matrix, which, in turn, leads to a reduction in pore size. This phenomenon ultimately culminates in a higher proportion of CaO_4Si hydrate formation, reinforcing the concrete's overall durability [3].

Enhancing the resistances and durability of the materials can further reduce pollution by lowering their carbon emission and the energy required during usage. The cleanup of the environment will be helped by the nano materials used on the building's structural components [4]. The material characteristics at the nano scale are drastically different from those at bigger scales due to the size of the nano particles [5]. The introduction of both nano-sized and micro-sized silica particles led to a substantial reduction in both initial and final setting times. Simultaneously, there was a remarkable enrich in the compressive strength of the hardened cement paste, with the most pronounced effects observed after a seven-day curing period [6]. These results underscore

the considerable potential of incorporating nano-sized and micro-sized silica particles in enhancing the early strength development and setting characteristics of OPC pastes [7].

The study revealed a notable boost in the cement mortar's compressive strength, with increases ranging from 1% to 20% in comparison to combinations without nano-silica. These results highlight the significant potential of nanoparticles to improve cement-based material performance [8]. The central focal point of this investigation rested upon scrutinizing the microstructure and morphology of cement composites wherein Graphene Oxide (GO) nanoparticles had been seamlessly integrated [9]. Two significant studies in FE-SEM and unveiled valuable insights. Their research outcomes highlighted the presence of hydroxyl, epoxide, and carbonyl functional groups on Graphene Oxide (GO) nanoparticles. These functional groups exhibit a remarkable capacity to establish covalent bonds with key components such as C-S-H and $\text{Ca}(\text{OH})_2$ within cementitious materials [10].

The replacement percentages for cement with SF ranged from 2.5% to 12.5%. However, it's worth noting that a decline in these properties was observed at the 7.5% replacement level. This decline can be attributed to the pronounced pozzolanic nature of SF, where compressive strength is particularly influenced by the rate at which silica fume forms the C-S-H gel [11]. At different weight percentages of the cement—that is, 0%, 5%, 10%, 15%, and 20%—silica fume was added to replace some of the cement. As per the study results, the range of 10% to 15% was found to be the ideal replacement level of SF for cement in order to get the maximum compressive strength after 21 days [12]. In this particular blend, there were remarkable enhancements observed in both the compressive and flexural strength of the mortar, signifying the potential for NS to substantially bolster the mechanical properties of cement-based materials. The acceleration of the hardening process in the presence of NS [13].

Introducing GO into cement paste and concrete. They particularly emphasize that the substantial specific surface area of GO can lead to an increase in viscosity, potentially hindering the workability and fluidity of the cement mixture. This issue has the potential to impose limitations on the practical incorporation of GO in concrete technology [14]. The usage of GO and carbon nanotubes (CNTs) together boosts the cement matrix's flexural strength by 72.7%, compared to gains of 51.2% and 26.3% when CNTs were employed alone [15]. The study showed significant improvements in the material's characteristics after 28 days of hydration, including an astounding rise in flexural strength of around 90.5% and compressive strength of about 40.4%. These results demonstrate graphene oxide's (GO) enormous potential as a reinforcing ingredient in cement-based composites. The enhancement of these materials' physical qualities by GO is indicated by the improvements in flexural and compressive strengths [16].

2. FLEXURAL PERFORMANCE

In our comprehensive investigation, we conducted a meticulous assessment of the flexural performance exhibited by concrete beams, employing a rigorous static load testing procedure. The concrete beams in question were of precise dimensions, measuring 1200 mm × 150 mm × 150 mm, and were subjected to a precisely controlled loading regimen [17, 18]. The overarching goals of this test encompassed the measurement of vital parameters that are pivotal in understanding the beam's behavior under bending stresses. These parameters included load-deflection characteristics, the initiation of the first crack, the development of ultimate cracks, and an assessment of the beam's energy absorption capacity. The insights garnered from this testing regime hold immense significance as they offer a deep understanding of the structural performance and load-bearing capabilities of the concrete beam when subjected to bending forces. This knowledge is indispensable for the assessment of the beam's suitability for real-world applications and plays a pivotal role in informing structural design decisions.

3. EXPERIMENTAL INVESTIGATION

3.1. Load – deflection behavior

A hydraulic jack was employed to apply loading up to 5 kN, and various measurements, including deflections and strains, were observed at both loading points and the mid-point of the beam [19, 20]. Data collection occurred at 5 kN load increments, capturing load deflections and strain values for both the initial crack and ultimate load stages. Using deflectometers fixed at the beam's bottom, vertical deformations at mid-span and two load points were recorded. The demountable mechanical strain gauge (DEMEC) with a precision of 0.001 mm was employed for strain measurements at different load levels. Throughout the testing, crack patterns were carefully marked during each loading interval. Additionally, the study documented the number of cracks that developed, crack spacing, and the height of crack propagation from the beam's bottom at each load interval. The comprehensive recording of these parameters provides a detailed understanding of the beam's behavior under varying loads, ensuring a thorough and accurate analysis of the structural response.

3.2. Ductility characteristics

The presented results and discussion pertain to the ductility factors and cumulative ductility factors (Cum. Ductility Factor) obtained for six different samples (M1 to M6) subjected to varying levels of load (P) in kiloneutons (kN) [21]. Ductility is a vital parameter in structural engineering, as it indicates the ability of a material or structure to deform and absorb energy without experiencing catastrophic failure. The ductility factor, in this context, measures the displacement of the material or structure relative to its original length. Upon analyzing the data, it is evident that as the applied load (P) increases, the ductility factor decreases for all six samples. This decrease in ductility suggests that the materials or structures become less capable of deformation as the load intensifies, which is a typical behavior observed in structural engineering. Therefore, the cumulative ductility factor shows the total deformation experienced by each sample as the load is incrementally increased. It is clear that as the load increases, the cumulative ductility factor accumulates, indicating the total deformation the material or structure undergoes.

3.3. Stiffness characterization

In flexural behavior, stiffness characterisation entails methodically assessing a material's rigidity and deformation response to applied stresses [22]. Standardized specimens are prepared, an exact testing device is assembled, and incremental loads are applied while corresponding deformations are recorded. Accurate measurement of the material's reaction is ensured by the apparatus, which includes displacement transducers. The yield point and other key points may be found and the initial stiffness can be calculated by an analysis of the load-deformation curve. This thorough process offers crucial information on the flexural performance of the material, assisting in the evaluation of its resilience and structural integrity under various loads.

3.4. Energy absorption capacity

Energy absorption capacity refers to the ability of a material or structure to absorb and dissipate energy under an applied load. In the context of flexural behavior, it is a measure of how much energy a material can absorb before experiencing failure or deformation. This capacity is often assessed by analyzing the area under the load-deformation curve obtained from flexural testing. A higher energy absorption capacity indicates better resilience and ductility of the material, as it can absorb more energy before reaching a vital point. This parameter is crucial in evaluating the performance and safety of materials in structural applications, providing insights into their ability to withstand dynamic loads and deformations without catastrophic failure.

3.5. Energy index

The energy index in the context of materials or structures typically refers to a quantitative measure of the energy absorption or dissipation capabilities. It is often derived from the area under the load-deformation curve obtained during mechanical testing, such as flexural testing. The energy index is a comprehensive metric that considers the entire loading and unloading phases, providing insights into the material's ability to absorb and release energy during deformation. A higher energy index suggests greater resilience and the capacity to withstand dynamic loads. This parameter is significant in assessing the overall performance and durability of materials, particularly in applications where energy absorption and dissipation are vital factors, such as in structures subjected to impact.

3.6. Finite element analysis (ANSYS)

The finite element analysis program ANSYS is used to examine structural elements such as beams, trusses, slabs, frames, and domes. The unique outcomes that are not achievable in the experimental inquiry are simulated using ANSYS. ANSYS software is specifically used to study the non-linear behavior of the concrete slab part. The concrete slab element is investigated numerically using ANSYS workbench and ANSYS parametric design language (APDL). The user interface of ANSYS Workbench is simpler than that of APDL. However, it serves as the basis for all the intricate aspects. APDL provides a quick overview of the graphical user interface, APDL command syntax, and APDL workflow. This information facilitates understanding of the structural component analysis virtual method.

Modeling a concrete beam with dimensions and characteristics that matched experimentally tested beams was part of the FEA calibration research. The ANSYS DESIGN MODELER environment was used to create the reinforcement (1D model) using concept tool and the concrete model (3D model) using extrude tool, as shown in figures 1(a) and 1(b). Completing these tasks is necessary for the finite element model in ANSYS WORKBENCH R14.5 to function correctly.

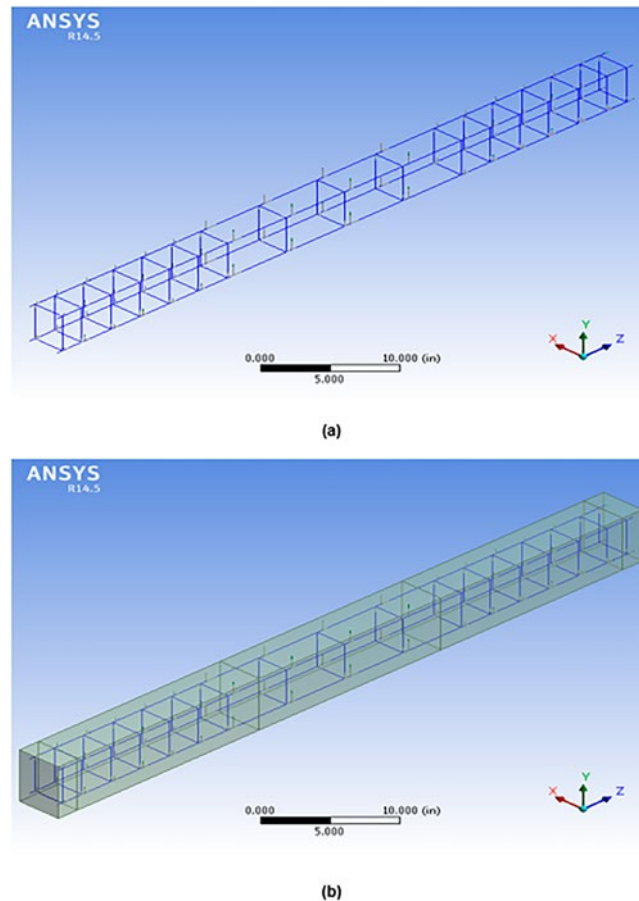


Figure 1: 3D model by using extrude tool.

4. RESULTS AND DISCUSSION

4.1. Load – deflection behavior

The structural response of the system to increasing applied loads (P) at different locations along its span. As the load magnitude rises from 0 kN to 105 kN, a clear trend emerges. The deflections (δ) at all six measurement points (M1 through M6) gradually increase. This observation is consistent with the fundamental principles of structural mechanics, where higher loads lead to increased deformations. Initially, at lower loads, the deflections remain relatively small and linear, with a predictable response across all measurement points. However, as the load surpasses 60 kN, a notable nonlinear behavior is observed, with deflections increasing more rapidly. This nonlinear response could be attributed to factors such as material yielding or structural instability, which need to be further investigated. It is evident that the deflections at different measurement points vary. This variance is due to the distribution of loads and moments along the structure's length, resulting in differential deformations. The experimental results provide valuable insights into the behavior of the tested structure under increasing loads. The reason for low deflection is addition of graphene oxide in concrete, upto 0.04% of graphene oxide the deflection is less and further increase in GO increase in pore holes thus deflection in more. Figure 2 shows the load vs. deflection curves of all mix (M1 to M6).

4.2. Ductility characteristics

The ductility factor values for specimens M1 to M6 at a load of 105 kN. Ductility factors, calculated as the ratio of maximum displacement to yield displacement, provide insights into the deformation capacity and flexibility of each specimen under the applied load. The results indicate that M5 has the highest ductility factor at 3.33, suggesting greater deformation capacity and flexibility compared to the other specimens. In contrast, M4 exhibits the lowest ductility factor at 3.41, indicating relatively less deformation under the applied load. These findings contribute to a comprehensive understanding of the structural behavior and deformation characteristics of each specimen, offering valuable information for assessing the ductile performance of concrete elements in response to external loads. Figure 3 shows the ductility factor of mix M1 to M6 at 105 kN.

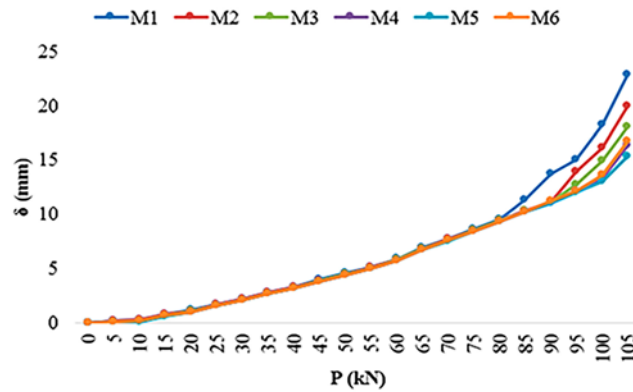


Figure 2: Shows the load vs. deflection curves of all mix (M1 to M6).

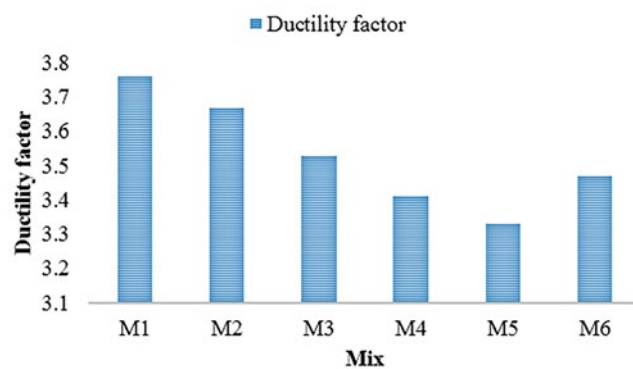


Figure 3: Shows the ductility factor of mix M1 to M6 at 105 kN.

4.3. Stiffness characterization

The stiffness factor values for specimens M1 to M6 at a load of 105 kN. Stiffness factor, expressed in kN/mm, represents the ratio of applied load to the corresponding displacement, providing insights into the material's rigidity. The results indicate varying stiffness among the specimens, with M1 having the highest stiffness factor at 17.5 kN/mm and M5 exhibiting the lowest at 15 kN/mm. These values characterize the materials' ability to resist deformation under the specified load, offering vital information for understanding and comparing the flexural behavior of each specimen. Figure 4 shows the stiffness factor of mix M1 to M6.

4.4. Energy absorption capacity

The assessment of concrete specimen energy absorption capacity was conducted across diverse loading conditions denoted by the applied force (P in kN). The tabulated results for six distinct mixes (M1 to M6) shed light on their respective performances regarding energy absorption. Notably, Mix M5 emerges as the frontrunner, displaying the highest energy absorption capacity at 2460 kNmm under a 105 kN force. This underscores Mix M5's exceptional capability to absorb and dissipate energy during loading. Additionally, Mix M2 and Mix M3 exhibit noteworthy energy absorption capacities, registering 1960 kNmm and 1940 kNmm, respectively. Disparities in energy absorption across the mixes are attributed to variations in composition and material properties, emphasizing the pivotal role of mix design in shaping the structural response and energy absorption characteristics of the concrete specimens. Figure 5 shows the energy absorption of mix M1 to M6.

4.5. Energy index

At a force of 105 kN, the concrete specimens' Energy Index was assessed to see how well each mix (M1 through M6) performed in terms of energy efficiency. The figure 6 displays the results, which show that the mixtures' respective Energy Index values differ. With the highest Energy Index of 10.69, Mix M5 stands out as having exceptional efficiency when it comes to absorbing and using energy under the given stress. Excellent Energy Index values of 10.0 and 10.23 are likewise shown by Mixes M4 and M6. These adjustments demonstrate how material characteristics and mix composition affect the concrete sample's energy performance. The Energy Index

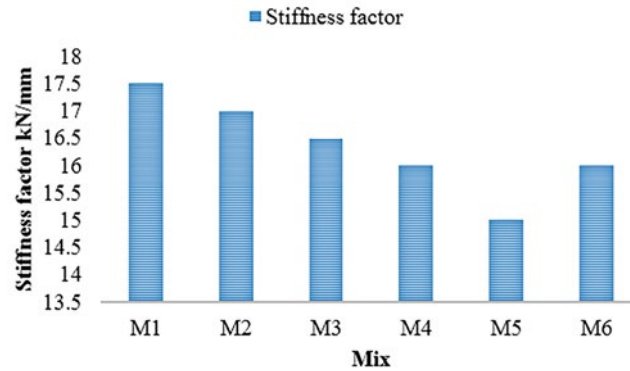


Figure 4: Shows the stiffness factor of mix M1 to M6.

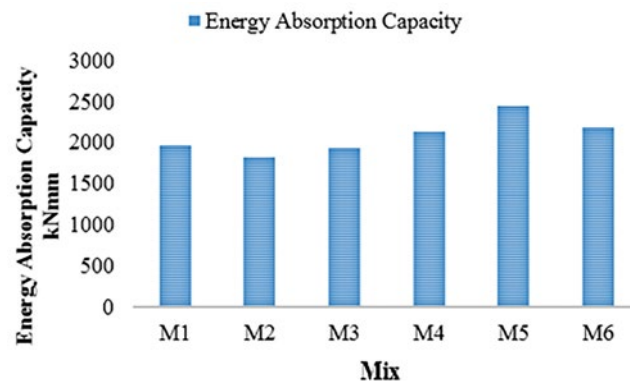


Figure 5: Shows the energy absorption of mix M1 to M6.

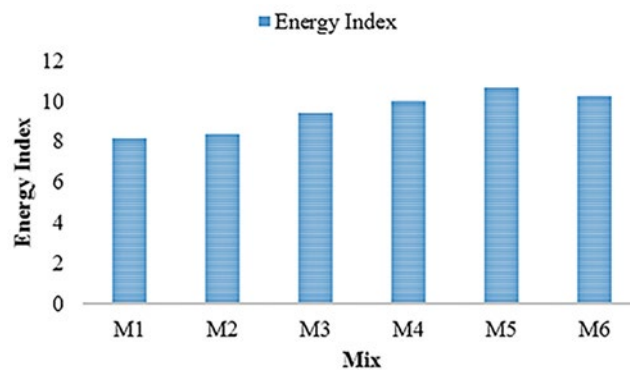


Figure 6: Shows the energy index off mix M1 to M6.

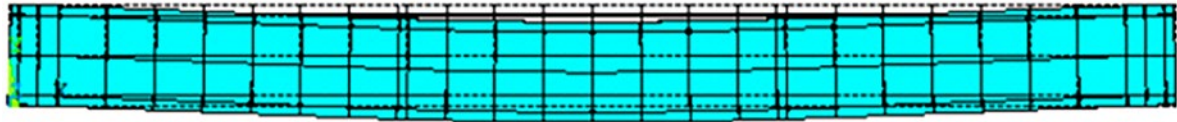
contributes to a thorough knowledge of the behavior of the material under loading circumstances by offering insightful information about how well each mix optimizes energy absorption and use.

4.6. Finite element analysis

The presented table illustrates the comparison between experimental (EXP.) and Finite Element Analysis (FEA) results for a series of applied loads (P) in kilonewtons (kN). The experimental data indicates the actual observed values during testing, while FEA provides simulated and calculated values. Across the range of loads, there is a generally close correlation between the experimental and FEA results, signifying the accuracy of the simulation in predicting the structural response. Discrepancies may be attributed to factors such as material properties, boundary conditions, or assumptions made in the simulation. This comparative data is crucial for validating the accuracy and reliability of the Finite Element Analysis in simulating the flexural behavior of the structure under varying loads. Figures 7 and 8 shows the deflection of M4 mix concrete beam under static load by ANSYS

DISPLACEMENT

STEP= 1
 SUB = 100
 TIME= 1
 DMX = 9.25



STATIC

Figure 7: Shows the deflection of M4 mix beam by static load test using ANSYS.

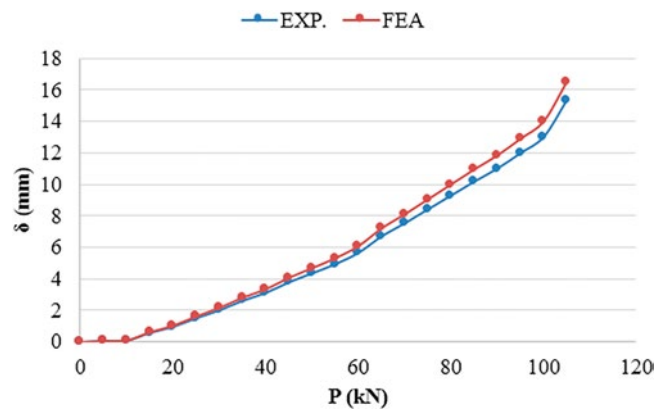


Figure 8: Comparison of flexural behavior and FEA (ANSYS) under static load test.

software and comparison of load deflection curve for FEA and flexural performance of concrete by using static load test.

5. CONCLUSION

In this research, the percentage of fly ash and silica fume is consistently maintained at 10% each as partial replacements for cement. Additionally, graphene oxide (GO) is introduced at varying percentages, from 0 to 0.05%, to study its impact on the flexural behavior of high-strength concrete (M60 grade). Experimental investigations were conducted on reinforced concrete (RC) beams subjected to monotonic loading, and the resulting structural behavior of all concrete mixes was analyzed and compared with finite element analysis (FEA) using ANSYS. The inclusion of graphene oxide significantly enhanced the performance metrics of the RC beams. Notably, the stiffness of the reinforced concrete beam elements improved by 14.28%, reflecting a substantial increase in their resistance to deformation. The ductility factor, a measure of a beam's capacity to undergo deformation under load, increased by 11.43%, while the energy absorption capacity improved by 25.51%, indicating enhanced resilience. The energy index, a parameter measuring the total energy absorbed before failure, saw an improvement of 30.84%. The addition of graphene oxide effectively transformed high-strength concrete into high-performance concrete, enabling it to exhibit superior structural behavior under both static and dynamic loading conditions. The load-deflection curves from experimental testing closely matched those generated by finite element analysis, affirming the accuracy of the FEA model in simulating the behavior of graphene oxide-enhanced concrete elements under applied loads. This study underscores the potential of graphene oxide to significantly improve the performance of concrete in structural applications.

6. BIBLIOGRAPHY

- [1] SILVESTRE, J., SILVESTRE, N., DE BRITO, J., “Review on concrete nanotechnology”, *European Journal of Environmental and Civil Engineering*, v. 20, n. 4, pp. 455–485, 2016. <http://doi.org/10.1080/19648189.2015.1042070>.
- [2] ARASU, A., NATARAJAN, M., BALASUNDARAM, N., *et al.*, “Utilizing recycled nanomaterials as a partial replacement for cement to create high-performance concrete”, *Global NEST Journal*, v. 25, n. 6, pp. 89–92, 2023.
- [3] LUO, Q., XIANG, Y., YANG, Q., *et al.*, “Molecular simulation of calcium-silicate-hydrate and its applications: a comprehensive review”, *Construction & Building Materials*, v. 409, pp. 134137, 2023. <http://doi.org/10.1016/j.conbuildmat.2023.134137>.
- [4] HAN, B., LI, Z., ZHANG, L., *et al.*, “Reactive powder concrete reinforced with nano SiO₂-coated TiO₂”, *Construction & Building Materials*, v. 148, pp. 104–112, 2017. <http://doi.org/10.1016/j.conbuildmat.2017.05.065>.
- [5] PARTHASAARATHI, R., BALASUNDARAM, N., NAVEEN ARASU, A., “A stiffness analysis of treated and non-treated meshed coir layer fibre reinforced cement concrete,” *AIP Conference Proceedings*, vol. 2861, no. 1, pp. 050002, 2023. <http://doi.org/10.1063/5.0158672>.
- [6] MONTGOMERY, J., “Effect of nano silica on the compressive strength of harden cement paste at different stages of hydration”, M.Sc. Thesis, North Carolina Agricultural and Technical State University, North Carolina, 2015.
- [7] LI, L.G., HUANG, Z.H., ZHU, J., *et al.*, “Synergistic effects of micro-silica and nano-silica on strength and microstructure of mortar”, *Construction & Building Materials*, v. 140, pp. 229–238, 2017. <http://doi.org/10.1016/j.conbuildmat.2017.02.115>.
- [8] ARASU, A.N., MUTHUSAMY, N., NATARAJAN, B., *et al.*, “Optimization of high performance concrete composites by using nano materials,” *Research on Engineering Structures and Materials*, v. 9, no. 3, pp. 843–859, 2023.
- [9] PALERMO, V., KINLOCH, I.A., LIGI, S., *et al.*, “Nanoscale mechanics of graphene and graphene oxide in composites: a scientific and technological perspective”, *Advanced Materials*, v. 28, n. 29, pp. 6232–6238, 2016. <http://doi.org/10.1002/adma.201505469>. PMID:26960186.
- [10] REHMAN, K.U., SARDAR, Z.I., MEMON, S.A., *et al.*, “Influence of graphene nanosheets on rheology, microstructure, strength development and self-sensing properties of cement based composites”, *Sustainability*, v. 10, n. 3, pp. 822, 2018. <http://doi.org/10.3390/su10030822>.
- [11] FAHMY, M.A., ABU EL-HASSAN, M.M., KAMH, G.M., *et al.*, “Investigation of using nano-silica, silica fume and fly ash in high strength concrete,” *Engineering Research Journal*, v. 43, n. 3, pp. 211–221, 2020.
- [12] KUMAR, S.N., NATARAJAN, M., NAVEEN ARASU, A., “A comprehensive microstructural analysis for enhancing concrete’s longevity and environmental sustainability”, *Journal of Environmental Nanotechnology*, v. 13, n. 2, pp. 368–376, 2024. <http://doi.org/10.13074/jent.2024.06.242584>.
- [13] HODHOD, O.A., KHALAFALLA, M.S., OSMAN, M.S.M., “ANN models for nano silica/silica fume concrete strength prediction”, *Water Science*, v. 33, n. 1, pp. 118–127, 2019. <http://doi.org/10.1080/11104929.2019.1669005>.
- [14] MOWLAIEI, R., LIN, J., BASQUIROTO DE SOUZA, F., *et al.*, “The effects of graphene oxide-silica nanohybrids on the workability, hydration, and mechanical properties of Portland cement paste”, *Construction & Building Materials*, v. 266, pp. 121016, 2021. <http://doi.org/10.1016/j.conbuildmat.2020.121016>.
- [15] ARASU, A.N., NATARAJAN, M., BALASUNDARAM, N., *et al.*, “Development of high-performance concrete by using nanomaterial graphene oxide in partial replacement for cement”, *AIP Conference Proceedings*, vol. 2861, pp. 050008, 2023.
- [16] ZHOU, C., LI, F., HU, J., *et al.*, “Enhanced mechanical properties of cement paste by hybrid graphene oxide/carbon nanotubes”, *Construction & Building Materials*, v. 134, pp. 336–345, 2017. <http://doi.org/10.1016/j.conbuildmat.2016.12.147>.
- [17] SRINIVASAN, S.S., MUTHUSAMY, N., ANBARASU, N.A., “The structural performance of fiber-reinforced concrete beams with nanosilica”, *Matéria (Rio de Janeiro)*, v. 29, n. 3, pp. e20240194, 2024. <http://doi.org/10.1590/1517-7076-rmat-2024-0194>.

- [18] PARTHASAARATHI, R., BALASUNDARAM, N., ARASU, N., “Analysing the impact and investigating Coconut Shell Fiber Reinforced Concrete (CSFRC) under varied loading conditions”, *Journal of Advanced Research in Applied Sciences and Engineering Technology*, v. 35, n. 1, pp. 106–120, 2024.
- [19] SHANKAR, S.S., NATARAJAN, M., ARASU, A., “Exploring the strength and durability characteristics of high-performance fibre reinforced concrete containing nanosilica”, *Journal of the Balkan Tribological Association*, v. 30, n. 1, pp. 142–152, 2024.
- [20] GANAPATHY, G.P., ALAGU, A., RAMACHANDRAN, S., *et al.*, “Effects of fly ash and silica fume on alkalinity, strength and planting characteristics of vegetation porous concrete”, *Journal of Materials Research and Technology*, v. 24, pp. 5347–5360, 2023. doi: <https://doi.org/10.1016/j.jmrt.2023.04.029>.
- [21] KADHAR, S.A., GOPAL, E., SIVAKUMAR, V., *et al.*, “Optimizing flow, strength, and durability in high-strength self-compacting and self-curing concrete utilizing lightweight aggregates”, *Matéria (Rio de Janeiro)*, v. 29, n. 1, pp. e20230336, 2024. doi: <http://doi.org/10.1590/1517-7076-rmat-2023-0336>.
- [22] GANAPATHY, G.P., KALIYAPPAN, S.P., RAMAMOORTHY, V.L., *et al.*, “Low alkaline vegetation concrete with silica fume and nano-fly ash composites to improve the planting properties and soil ecology”, *Nanotechnology Reviews*, v. 13, n. 1, pp. 20230201, 2024. doi: <http://doi.org/10.1515/ntrev-2023-0201>.